The Effect of Interfacial Deformation on Electrodeposition Kinetics

Journal of The Electrochemical Society, **151** (6) A880-A886 (2004)
0013-4651/2004/151(6)/A880/7/$7.00 © The Electrochemical Society, Inc.

The Effect of Interfacial Deformation on Electrodeposition Kinetics

Charles Monroe*,z and John Newman**

Department of Chemical Engineering, University of California, Berkeley, California 94720-1462, USA

Mullins-Sekerka linear stability analysis and the Barton and Bockris dendrite-propagation model are popular methods used to describe cathodic roughening and dendritic growth. These commonly cited theories employ kinetic relationships that differ in mathematical form, but both contain the effects of surface tension and local concentration deviations induced by surface roughening. Here, a kinetic model is developed which additionally includes mechanical forces such as elasticity, viscous drag, and pressure, showing their effect on exchange current densities and potentials at roughening interfaces. The proposed expression describes the current density in terms of applied overpotential at deformed interfaces with arbitrary three-dimensional interfacial geometry. Both the Mullins-Sekerka and the Barton-Bockris kinetics can be derived as special cases of the general expression, thereby validating the proposed model and elucidating the fundamental assumptions on which the two previous theories rely.
 [DOI: 10.1149/1.1710893]

Manuscript received May 27, 2003. Available electronically May 4, 2004.

Dendrite formation is a primary failure mechanism in lithium/polymer batteries. While such deposits were first hypothesized to occur in lithium/organic systems in 1974,[1] and first directly observed in 1980,[2] the experimental and theoretical examination of morphological instability during thermal and electrochemical deposition has a rich history that extends back to the 1960s.[3,4] Studies typically divide the electrochemical dendrite problem into two main parts: the initiation regime, in which an initially regular cathode surface begins to form irregularities, and the propagation regime, in which nucleated deposits begin to grow away from the cathode, into the bulk electrolyte.[4] It is from the treelike appearance of deposits in the second regime that ''dendrites'' derive their name.

There are three theories commonly used to describe the velocity of electrochemical dendrite propagation. In diffusion-limited aggregation models, random-walk statistics is employed to develop the fractal shapes and extension rates of mass-transfer-limited deposits.[5,6] Migration-limited mass-transfer models suggest that violation of electroneutrality near dendrite tips leads to high overpotentials, fostering extension of surface irregularities toward the counter electrode.[7] In surface-tension mitigated growth, an increased curvature of the dendrite tip is hypothesized to balance large mass-transfer driving forces incurred by the low concentration of cations near dendrite surfaces.[8]

The most applicable fractal propagation model is that developed by Chen and Jorné;[9] migration-limited mechanisms are described in the work of Chazalviel.[7] Both approaches rely on the assumption that high voltages (*ca.* 10 V) are applied to the electrochemical cell. This high-voltage restriction corresponds to cell currents well over the limiting value. Though these models may provide informative mechanistic arguments at high currents, they should not be applied to secondary-battery systems run under practical charging conditions.

The Barton and Bockris model of propagation,[8] later improved by Diggle *et al.*,[10] describes growth in well-supported electrolytes, calling into question its applicability to polymer electrolyte systems. In addition, the model assumes that propagating dendrite tips are relatively isolated and hemispherical in shape. However, the Barton and Bockris approach is able to describe dendrite propagation far below limiting currents. Recent observation of such behavior *in situ* in the lithium/polymer system[11] makes this model particularly appealing. The treatment has been extended to systems containing a diffusion boundary layer near the cathode by Oren and Landau; their study shows excellent comparison to experiment and concludes, in the case of liquid electrolytes, that the propagation model can be extended to amplification of surface irregularities in the boundary layer.[12] Recent modeling work by the authors of this paper[13] extends the Barton and Bockris model to unsupported electrolytes, which yield similar propagation behavior to the well-supported systems described by Diggle *et al.*[10]

Whether above or below the limiting current, each theoretical propagation study listed suggests that dendrite growth cannot be prevented once a system has reached the propagation regime. Therefore, analysis of initiation phenomena remains the only available route to find conditions which prevent dendrite formation. Two approaches, one statistical and one continuum-scale, theoretically rationalize the initiation mechanism.

A statistical approach to dendrite initiation is taken by Deutscher and Fletcher, who use a simple probabilistic nucleation model to relate the rate of appearance of nucleated crystals to a number of active nucleation sites and an activation rate parameter.[14] One great success of this theory is that it can be used to deconvolute the seemingly random current *vs.* time (or potential *vs.* time) behavior characteristic of systems exhibiting dendritic deposits, allowing determination of nucleation rates from noisy current-time transient measurements.[15] While effective for data analysis and useful to describe experimental behavior qualitatively, the parameters used in Deutscher-Fletcher nucleation theory do not correspond to bulk material properties and cannot be used to predict experimental circumstances that may inhibit dendrite formation.

Linear stability analyses are phenomenological treatments of irregular diffusional deposition; they incorporate independently measurable material properties. These analyses typically parallel the original development by Mullins and Sekerka, who developed stability criteria in one-dimensional thermal systems where surface-tension forces slow the rate of solid deposition from melts.[16,17] The Mullins-Sekerka method was extended to unsteady galvanostatic deposition from a two-dimensional semi-infinite region by Aogaki and Makino[18] and was further extended by Aogaki,[19] who compares results of a three-dimensional, semi-infinite stability analysis to scanning electron micrographs of real interfaces. An excellent brief summary of further linear stability work is given by Sundström and Bark; their paper also contributes two-dimensional solutions which determine the effects of finite geometry in parallel-electrode cells and suggests an avenue of attack in the three-dimensional finite problem.[20] Each of the electrochemical stability analyses discussed shows universal instability, *i.e.*, dendrite growth occurs at the cathode for all values of applied current.

The literature regarding cathodic stability in stagnant electrolytes is abundant and discouraging. At this point, the Mullins-Sekerka approach has been generalized to realistic geometric situations with no signs of stable growth regimes, suggesting that morphological instabilities at the cathode may be practically insurmountable. However, in polymer electrolyte systems, and particularly in the partially cross-linked polymer electrolytes currently in development,[21] new questions and situations are posed.

* Electrochemical Society Active Member.
** Electrochemical Society Fellow.
z E-mail: cwmonroe@newman.cchem.berkeley.edu

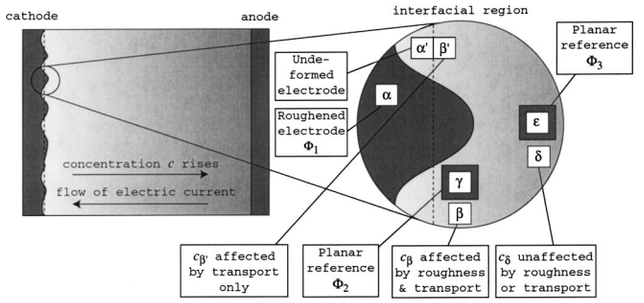

Figure 1. Schematic diagram of the macroscopic cell geometry and various phases required for theoretical description of the interfacial region. (— — —) An undeformed interfacial position.

Mullins-Sekerka initiation analysis, like the Barton and Bockris propagation theory, assumes that surface tension is the sole factor resisting morphological instability. If effects other than surface forces, such as elastic or viscous forces, can be exploited in practical systems, it may be possible to obtain cathodic morphological stability. To that end, we develop a general kinetic framework which includes the effects of external pressure, elastic deformation, and viscous stress effects in addition to the surface tension. In developing this framework, we show that it is consistent with models already employed in the literature and clarify some of the assumptions implicitly made in linear stability analysis and dendrite propagation modeling.

Thermodynamic Relationships

Our theoretical approach must begin with an idealized description of the various phases to be analyzed. A schematic diagram of the system we consider is shown in Fig. 1. The figure shows a one-dimensional parallel-electrode electrochemical cell some time after the application of a constant current. After some current has passed, we expect that the anode remains relatively smooth and the cathode may roughen; the undeformed interfacial position, its position before current is applied, is indicated in the figure by finely dotted lines. The inset shows thermodynamic phases required for description of the interfacial region. Phases α' and β' represent undeformed solid and electrolyte, respectively. Phase α is the electrode surface, which may be slightly deformed; phase β is the electrolyte close to the roughening surface, where salt concentration c is affected by roughening of the interface; and phase δ is a region in the vicinity of the surface, sufficiently distanced so that the concentration profile matches the behavior yielded by solution of the one-dimensional macroscopic transport equations. Phases γ and ε are planar reference electrodes of a given kind in regions β and δ, respectively.

Equilibrium conditions across the undeformed surface are given by the two equations

$$p^{\alpha'} = p^{\beta'} \qquad [1]$$

$$\mu_M^{\alpha'} = \mu_{M^{z+}}^{\beta'} + z_+\mu_{e^-}^{\alpha'} \qquad [2]$$

where p is the pressure, z_+ is the valence of the cation, and μ_i is the electrochemical potential of reactant species i; M denotes the reacting metal, M^{z+} is the cation, and e^- represents an electron. Across a deformed interface, we must relax the pressure condition. Equilibrium is then defined solely by

$$\mu_M^{\alpha} = \mu_{M^{z+}}^{\beta} + z_+\mu_{e^-}^{\alpha} \qquad [3]$$

where the primes have been dropped on the superscripts to denote the deformed condition.

To find the effect of deformation on the equilibrium condition, we assume that the electrochemical potentials of electrons depend on the absolute temperature T and the quasi-electrostatic potential Φ

$$\mu_{e^-} = \mu_{e^-}(T,\Phi) \qquad [4]$$

and those of all remaining species depend on temperature, pressure, and composition according to

$$\mu_i = \mu_i(T,p,c_M,c_S,c_{M^{z+}},c_{X^{z-}}) \qquad [5]$$

where p is the external pressure. Species concentrations are reflected by c_i; a subscript S represents solvent and X^{z-} the anion. When the electrode, which contains metal and electrons, but no ions, is deformed at constant temperature, the total differential of electrochemical potential in the metal is

$$d\mu_M = \left(\frac{\partial\mu_M}{\partial p}\right)_{T,c_M} dp + \left(\frac{\partial\mu_M}{\partial c_M}\right)_{T,p} dc_M \qquad [6]$$

In the electrolyte adjacent to the metal, we have

$$d\mu_i = \left(\frac{\partial\mu_i}{\partial p}\right)_{T,c_i} dp + \left(\frac{\partial\mu_i}{\partial c_{M^{z+}}}\right)_{T,p,c_j\neq c_{M^{z+}}} dc_{M^{z+}} + \left(\frac{\partial\mu_i}{\partial c_{X^{z-}}}\right)_{T,p,c_j\neq c_{X^{z-}}} dc_{X^{z-}} + \left(\frac{\partial\mu_i}{\partial c_S}\right)_{T,p,c_j\neq c_S} dc_S \qquad [7]$$

Under isothermal conditions, the chemical potential of electrons, μ_{e^-}, is a function only of the quasi-electrostatic potential Φ and can be found by employing Eq. 6 and 7 and equilibrium relationship Eq. 3.

Equations 6 and 7 can be simplified by inserting a standard constitutive relationship for the electrochemical potential[22]

$$\mu_i = RT\ln(f_i c_i a_i^{\theta}) \qquad [8]$$

where f_i is the molar activity coefficient of species i, c_i is its molar concentration, and a_i^{θ} is a property dependent on the secondary reference state of the system. The partial derivative with respect to pressure of the electrochemical potential of i is its partial molar volume

$$\left(\frac{\partial\mu_i}{\partial p}\right)_{T,c_i} = \overline{V}_i \qquad [9]$$

Using Eq. 6-9, we find that in a phase containing the neutral metal M

$$d\mu_M = \overline{V}_M dp + RT\left[1 + \left(\frac{\partial\ln f_M}{\partial\ln c_M}\right)_{T,p}\right] d\ln(c_M) \qquad [10]$$

and in an electrolyte phase containing ions but no M

$$d\mu_{M^{z+}} = \overline{V}_{M^{z+}}dp + RT\left[1 + \left(\frac{\partial\ln f_{M^{z+}}}{\partial\ln c_{M^{z+}}}\right)_{T,p,c_j\neq c_{M^{z+}}}\right] d\ln(c_{M^{z+}}) + RT\left[1 + \left(\frac{\partial\ln f_{X^{z-}}}{\partial\ln c_{X^{z-}}}\right)_{T,p,c_j\neq c_{X^{z-}}}\right] d\ln(c_{X^{z-}}) + RT\left[1 + \left(\frac{\partial\ln f_{X^{z-}}}{\partial\ln c_S}\right)_{T,p,c_j\neq c_S}\right] d\ln(c_S) \qquad [11]$$

Expressions 10 and 11 can be integrated to determine the electrochemical potential differences in M and M^{z+} due to roughening

$$\mu_M^{\alpha} - \mu_M^{\alpha'} = \int_{\alpha'}^{\alpha} \overline{V}_M dp + RT \int_{\alpha'}^{\alpha} \left[1 + \left(\frac{\partial \ln f_M}{\partial \ln c_M} \right)_{T,p} \right] d \ln(c_M) \quad [12]$$

$$\begin{aligned} \mu_{M^{z+}}^{\beta} - \mu_{M^{z+}}^{\beta'} = & \int_{\beta'}^{\beta} \overline{V}_{M^{z+}} dp \\ & + RT \int_{\beta'}^{\beta} \left[1 + \left(\frac{\partial \ln f_{M^{z+}}}{\partial \ln c_{M^{z+}}} \right)_{T,p,c_j \neq c_{M^{z+}}} \right] d \ln(c_{M^{z+}}) \\ & + RT \int_{\beta'}^{\beta} \left[1 + \left(\frac{\partial \ln f_{M^{z+}}}{\partial \ln c_{X^{z-}}} \right)_{T,p,c_j \neq c_{X^{z-}}} \right] d \ln(c_{X^{z-}}) \\ & + RT \int_{\beta'}^{\beta} \left[1 + \left(\frac{\partial \ln f_{M^{z+}}}{\partial \ln c_S} \right)_{T,p,c_j \neq c_S} \right] d \ln(c_S) \end{aligned} \quad [13]$$

Equations 12 and 13 generally describe the effects of deformation on electrochemical potentials, including the effect of compression on species concentrations.

When concentration changes due to volume strain are negligible, Eq. 12 and 13 can be rewritten as

$$\mu_M^{\alpha} - \mu_M^{\alpha'} = \int_{\alpha'}^{\alpha} \overline{V}_M dp \quad [14]$$

$$\mu_{M^{z+}}^{\beta} - \mu_{M^{z+}}^{\beta'} = \int_{\beta'}^{\beta} \overline{V}_{M^{z+}} dp \quad [15]$$

For small deformations to condensed phases, the assumption that molar volumes are unaffected by small deformations should also be reasonable. In this case, Eq. 14 and 15 can be integrated directly

$$\mu_M^{\alpha} - \mu_M^{\alpha'} = \overline{V}_M^{\alpha'} \Delta p^{\alpha,\alpha'} \quad [16]$$

$$\mu_{M^{z+}}^{\beta} - \mu_{M^{z+}}^{\beta'} = \overline{V}_{M^{z+}}^{\beta'} \Delta p^{\beta,\beta'} \quad [17]$$

Note that Eq. 16 and 17 introduce the shorthand notation

$$\Delta f^{i,j} = f^i - f^j \quad [18]$$

Subtracting equilibrium condition 2 from condition 3, and then inserting Eq. 16 and 17, we find that

$$\Delta \mu_{e^-}^{\alpha,\alpha'} = \frac{\overline{V}_M^{\alpha'}}{z_+} \Delta p^{\alpha,\alpha'} - \frac{\overline{V}_{M^{z+}}^{\beta'}}{z_+} \Delta p^{\beta,\beta'} \quad [19]$$

At equilibrium, the electrochemical potential difference between electrons in the deformed and undeformed condensed phases is related to the pressure differences incurred on either side of the interface by deformation.

The partial molar volume of cations cannot be obtained by direct measurement. It is more appropriate to relate the partial molar volume of cations to that of the neutral electrolyte salt, which can be obtained from the slope of a density/concentration curve. Employing the relationship proposed by Newman and Chapman,[23] which assumes that transference numbers of ions are inversely proportional to their partial molar volumes, we obtain

$$\overline{V}_{M^{z+}}^{\beta'} = \frac{t_-^0 \overline{V}_{M_{\nu_+}X_{\nu_-}}^{\beta'}}{\nu_+ (t_-^0 + t_+^0)} \quad [20]$$

where ν_+ and ν_- are the stoichiometric numbers of ions in a formula unit of the neutral salt, $\overline{V}_{M_{\nu_+}X_{\nu_-}}^{\beta'}$ is the partial volume of neutral salt, and t_+^0 and t_-^0 are the cationic and anionic transference numbers. Equation 20 leads to ionic partial molar volumes consistent with transport properties measured by the method of restricted diffusion.

Force Balance

Now we must relate the pressure differences from Eq. 19 to forces in bulk phases α and β. To perform this operation, we employ the definition familiar from mechanics that the force per unit area $\underline{F}$ acting on a plane with unit normal $\underline{e}_n$ is given by the equation

$$\underline{F} = \underline{e}_n \cdot \underline{\underline{\sigma}} \quad [21]$$

where $\underline{\underline{\sigma}}$ is the Cauchy stress,[24] defined here such that compressive stresses are positive.[25] For a force balance across the interface in question here, we require the relationship

$$\underline{e}_n^{\alpha} \cdot (\underline{\underline{\sigma}}^{\alpha} - \underline{\underline{\sigma}}^{\beta}) + \nabla_s \gamma - \gamma (\nabla_s \cdot \underline{e}_n^{\alpha}) \underline{e}_n^{\alpha} = 0 \quad [22]$$

where $\underline{e}_n^{\alpha}$ is the unit normal to phase α (pointing into phase β), γ is the surface energy, and the surface gradient ∇_s is defined as

$$\nabla_s \equiv (\underline{\underline{I}} - \underline{e}_n^{\alpha} \underline{e}_n^{\alpha}) \cdot \nabla \quad [23]$$

where $\underline{\underline{I}}$ is the identity tensor. In Eq. 22 interfacial acceleration and dilatational viscosity of the surface have been neglected for simplicity; a fully general form of this equation is given in the development by Scriven.[26] The surface divergence term in Eq. 22 is also commonly written in terms of the mean curvature of the surface, $\mathcal{H}$[27]

$$\mathcal{H} = -\frac{1}{2} \left(\frac{1}{r_1} + \frac{1}{r_2} \right) = -\frac{1}{2} (\nabla_s \cdot \underline{e}_n^{\alpha}) \quad [24]$$

where r_1 and r_2 are the principal radii of curvature at the interface. We assume that the surface energy is constant with respect to interfacial curvature; then Eq. 22 becomes

$$\underline{e}_n^{\alpha} \cdot (\underline{\underline{\sigma}}^{\alpha} - \underline{\underline{\sigma}}^{\beta}) + 2\gamma \mathcal{H} \underline{e}_n^{\alpha} = 0 \quad [25]$$

or, in terms of normal and tangential scalar components

$$\underline{e}_n^{\alpha} \cdot [\underline{e}_n^{\alpha} \cdot (\underline{\underline{\sigma}}^{\alpha} - \underline{\underline{\sigma}}^{\beta})] + 2\gamma \mathcal{H} = 0 \quad [26]$$

$$\underline{e}_t^{\alpha} \cdot [\underline{e}_n^{\alpha} \cdot (\underline{\underline{\sigma}}^{\alpha} - \underline{\underline{\sigma}}^{\beta})] = 0 \quad [27]$$

If the surface energy is constant with respect to curvature, physical values of the stresses in phases α and β must satisfy Eq. 26 and 27.

A general stress has deformational, viscous, and thermodynamic pressure components, according to the relationship

$$\underline{\underline{\sigma}} = \underline{\underline{\tau}}_d + \underline{\underline{\tau}}_v + p \underline{\underline{I}} \quad [28]$$

where $\underline{\underline{\tau}}_d$ is the deformation stress, $\underline{\underline{\tau}}_v$ is the viscous stress, and p is the external pressure. Substituting Eq. 28 into Eq. 26 and 27 yields

$$\underline{e}_n^{\alpha} \cdot \{\underline{e}_n^{\alpha} \cdot [(\underline{\underline{\tau}}_d^{\alpha} - \underline{\underline{\tau}}_d^{\beta}) + (\underline{\underline{\tau}}_v^{\alpha} - \underline{\underline{\tau}}_v^{\beta})]\} + (p^{\alpha} - p^{\beta}) + 2\gamma \mathcal{H} = 0 \quad [29]$$

$$\underline{e}_t^{\alpha} \cdot \{\underline{e}_n^{\alpha} \cdot [(\underline{\underline{\tau}}_d^{\alpha} - \underline{\underline{\tau}}_d^{\beta}) + (\underline{\underline{\tau}}_v^{\alpha} - \underline{\underline{\tau}}_v^{\beta})]\} = 0 \quad [30]$$

The pressure difference in Eq. 29 can be related to the electrochemical potential difference between electrons in roughened and planar surfaces.

The relationships developed thus far can be used to elucidate the relationships for electrochemical potential employed in the propagation literature. Combination of equilibrium conditions 2 and 3 and Eq. 16 and 17 gives

$$p^{\alpha} - p^{\beta} = \frac{z_+}{\overline{V}_M^{\alpha'}} \Delta \mu_{e^-}^{\alpha,\alpha'} + \left[\left(\frac{\overline{V}_{M^{z+}}^{\beta'}}{\overline{V}_M^{\alpha'}} \right) - 1 \right] \Delta p^{\beta,\beta'} \quad [31]$$

Substituting Eq. 31 into Eq. 29, and then rearranging, we obtain

$$\Delta\mu_{e^-}^{\alpha,\alpha'} = \frac{\overline{V}_M^{\alpha'}}{z_+}\left\{\left[\left(\frac{\overline{V}_{M^{z+}}^{\beta'}}{\overline{V}_M^{\alpha'}}\right) - 1\right]\Delta p^{\beta,\beta'} + 2\gamma\mathcal{H} + \underline{e}_n^{\alpha}\cdot[\underline{e}_n^{\alpha}\cdot(\Delta\underline{\underline{\tau}}_d^{\alpha,\beta} + \Delta\underline{\underline{\tau}}_v^{\alpha,\beta})]\right\} \quad [32]$$

Equation 32 expresses the electrochemical potential difference across a deformed interface in terms of the molar volumes of components when undeformed, the pressure acting on phase β after deformation, the surface energy, and the deformational and viscous stress differences across the interface. In cases when stress and compression of the electrolyte region are negligible (*e.g.*, for relatively slow deformation in a Newtonian fluid electrolyte, such as a dilute aqueous solution), and when the electrolyte is 1:1, Eq. 32 reduces to

$$\Delta\mu_{e^-}^{\alpha,\alpha'} = -2\gamma\overline{V}_M^{\alpha'}\mathcal{H} = \gamma\overline{V}_M^{\alpha'}\left(\frac{1}{r_1} + \frac{1}{r_2}\right) \quad [33]$$

which is the effect of surface tension on chemical equilibrium postulated by Barton and Bockris.[8] Equation 33 is analogous to the chemical potential relationships assumed to hold across interfaces in the theory of coalescing vapor droplets.[28]

Another more general relationship for the electrochemical potential difference across a deformed interface can be obtained by a slightly different rearrangement of Eq. 2, 3, 16, 17, and 29

$$\Delta\mu_{e^-}^{\alpha,\alpha'} = -\left(\frac{\overline{V}_M^{\alpha'} + \overline{V}_{M^{z+}}^{\beta'}}{2z_+}\right)\{2\gamma\mathcal{H} + \underline{e}_n^{\alpha}\cdot[\underline{e}_n^{\alpha}\cdot(\Delta\underline{\underline{\tau}}_d^{\alpha,\beta} + \Delta\underline{\underline{\tau}}_v^{\alpha,\beta})]\} + \left(\frac{\overline{V}_M^{\alpha'} - \overline{V}_{M^{z+}}^{\beta'}}{2z_+}\right)(\Delta p^{\alpha,\alpha'} + \Delta p^{\beta,\beta'}) \quad [34]$$

Equation 34 describes the change in electrochemical potential caused by mechanical forces around an isothermal roughening interface, including surface tension, elastic, plastic, and viscous response of the bulk phases, and externally applied pressures on the electrode or electrolyte. With the exception of the molar volumes and surface energy, which are thermodynamic material properties, all terms in Eq. 34 can be evaluated by obtaining solutions to the steady-state equation of motion.

Electrochemical Interfacial Kinetics

We seek to determine whether circumstances exist under which mechanical effects slow or suppress interfacial roughening during galvanostatic electrodeposition. Therefore, we must propose an expression to include the effect of deformation on kinetics of the redox reaction

$$M_{(s)}^0 \leftrightarrow M_{(sol'n)}^{z+} + z_+e_{(s)}^- \quad [35]$$

which occurs at the interface between phases α and β. The double-headed arrow indicates that Reaction 35 is considered reversible. For development of a kinetic equation, it is useful to break Eq. 35 into elementary steps

$$M_\alpha \leftrightarrow M_\alpha^{z+}\cdots z_+e_\alpha^- \overset{k_a}{\rightarrow} M_\beta^{z+} + z_+e_\alpha^- \quad [36]$$

$$M_\beta^{z+} + z_+e_\alpha^- \overset{k_c}{\rightarrow} M_\alpha^{z+}\cdots z_+e_\alpha^- \leftrightarrow M_\alpha \quad [37]$$

each of which passes through an identical intermediate species, $M_\alpha^{z+}\cdots z_+e_\alpha^-$. This intermediate is included to reflect that excitement of an electron from the valence to the conduction band of M (or vice versa) is a quasi-equilibrated step dependent on the applied potential and is not considered rate-limiting. Rather, the rate-limiting step is charge transfer to or from solution; adsorption and desorption kinetics of cations are lumped into the anodic and cathodic rate constants, k_a and k_c, respectively.

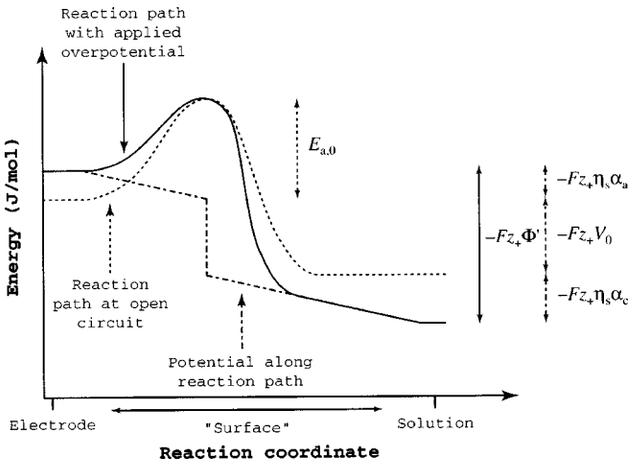

Figure 2. Plot of energy along the reaction path for an idealized redox reaction. (— — —) The reaction path at equilibrium and (——) with an applied overpotential, or when net current is passed. The electric potential profile across the surface is shown by the dash-dotted line.

To discuss electrochemical kinetics in the absence of deformation, we introduce an energy diagram along the reaction path shown in Fig. 2. In the figure, Φ' is the electric potential measured across the surface, which obeys the relationship

$$\Phi' = V_0 + \eta_s \quad [38]$$

where V_0 is the open-circuit (equilibrium) potential and η_s is the surface overpotential. The activation energy, $E_{a,0}$, quantifies the magnitude of the energy barrier to reaction at equilibrium. Figure 2 also shows the anodic and cathodic transfer coefficients α_a and α_c, which give the fractions of surface overpotential that go to lowering the anodic activation energy barrier and raising the cathodic activation energy barrier, respectively. The figure depicts a reaction scheme like that given in Eq. 36 and 37, namely, the cathodic reaction mechanism is the exact reverse of the anodic one, and the activated intermediate species in both directions is identical. We further assume that conditions can be obtained where surface adsorption is quasi-equilibrated, making charge transfer rate-limiting.

These mechanistic assumptions may be overly simple for transition metal or alloy electrode materials, which can pass through several electronic states as they react, or for electrodes that have rates limited by processes other than charge transfer to solution. Competitive reactions, such as formation of an oxide layer on the electrode or decomposition of the electrolyte, would also cause the situation to differ somewhat from the idealization depicted in Fig. 2. The existence of competitive reactions is also a primary concern in lithium-ion battery research;[29] because we wish to address electrode stability, we assume a practical system can be obtained in which such side reactions have been eliminated.

The combination of basic collision theory[30] and a reactant energy diagram such as Fig. 2 leads directly to a Butler-Volmer equation, which takes the general form

$$\frac{i}{z_+F} = k_a\exp\left(\frac{\alpha_a z_+F\Phi'}{RT}\right) - k_c a_{M^{z+}}\exp\left(-\frac{\alpha_c z_+F\Phi'}{RT}\right) \quad [39]$$

where i is the electric current density and $a_{M^{z+}}$ is the chemical activity of M^{z+}. Activity of M has been omitted from the anodic term in alignment with the earlier assumption that solid molar vol-

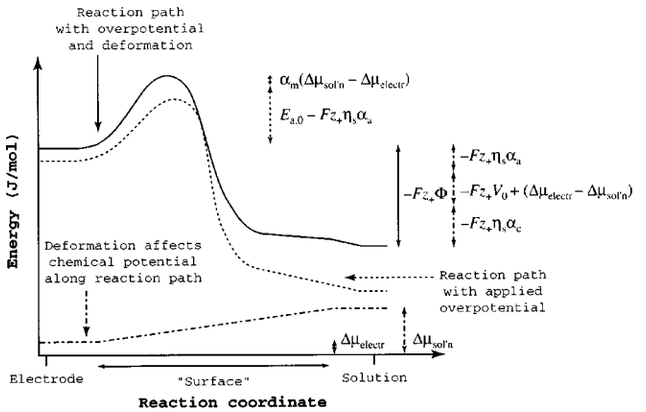

Figure 3. Reactant energy *vs.* reaction coordinate for a redox reaction, including effects of interfacial deformation. (— — —) The reaction path of a redox reaction with applied overpotential, also shown in Fig. 2; (——) the reaction path as affected by deformation. The profile of chemical potential change $\Delta\mu$ induced by deformation is shown by a dash-dotted line.

ume (the inverse of concentration in a pure phase) remains constant with deformation. If necessary, transition-state theory can provide additional arguments for the dependence of rate constants on molecular characteristics; here we ignore such further detail and treat k_a and k_c as practically measurable quantities. The exponential terms in Eq. 39 reveal how applied potentials affect the activation barrier in the anodic and cathodic directions. Values of transfer coefficients under the mechanistic assumptions listed can be related to the quantum-mechanical process of electron tunneling. Energetic arguments of the type employed here yield results identical to quantum theory if the activated complexes shown in Eq. 36 and 37, represented by the peak in Fig. 2, are interpreted to be at the electron-tunneling energy; for such reactions, quantum theory also concurs that transfer coefficients should sum to unity.[31]

We should modify Eq. 39 to include the deviations from chemical equilibrium incurred by interfacial deformation, which were derived in the previous section. To this end, we provide a schematic, Fig. 3, which adds the effects of deformation to the basic electrochemical picture, Fig. 2. The variables $\Delta\mu_{electr}$ and $\Delta\mu_{sol'n}$ reflect electrochemical potential differences due to deformation of the electrode and solution, respectively. An additional transfer coefficient α_m gives the fraction of the metal-solution electrochemical potential difference which contributes to the reaction activation energy. Note that the difference $\Delta\mu_{electr} - \Delta\mu_{sol'n}$ is the previously developed quantity

$$\Delta\mu_{electr} - \Delta\mu_{sol'n} = (\mu_M^{\alpha} - \mu_M^{\alpha'}) - (\mu_{M^{z+}}^{\beta} - \mu_{M^{z+}}^{\beta'}) = z_+\Delta\mu_{e^-}^{\alpha,\alpha'} \quad [40]$$

We reiterate that surface adsorption and side reactions have been neglected. Figure 3 and Eq. 40 provide a sufficient framework to propose a complete kinetic expression

$$\frac{i_n}{z_+F} = k_a \exp\left[\frac{\alpha_m z_+\Delta\mu_{e^-}^{\alpha,\alpha'}}{RT}\right]\exp\left(\frac{\alpha_a z_+F\Phi}{RT}\right) - k_c a_{M^{z+}} \exp\left[-\frac{(1-\alpha_m)z_+\Delta\mu_{e^-}^{\alpha,\alpha'}}{RT}\right]\exp\left(-\frac{\alpha_c z_+F\Phi}{RT}\right) \quad [41]$$

where i_n is the potential normal to the deformed electrode surface, and the potential across it is given by

$$\Phi = V_0 + \eta_s - \frac{\Delta\mu_{e^-}^{\alpha,\alpha'}}{F} \quad [42]$$

Equation 34 can now be used to incorporate stresses across and surface tension at an electrochemically reacting interface.

Our development allows a physical questioning of conditions commonly assumed in the dendrite literature. To take α_m equal to α_a in Eq. 41 follows from the assumption that mechanical forces solely affect equilibrium potentials, *i.e.*, the kinetic parameters are unaffected by deformation. This simplification is employed in the linear stability analyses of Aogaki,[18,19] Pritzker and Fahidy,[32] and Sundström and Bark.[20] Another way of describing the condition $\alpha_m = \alpha_a$ is to say that linear stability theories neglect the effect of deformation on the exchange current density.

To elucidate the kinetic expressions employed in propagation modeling requires a more convoluted derivation. Substituting Eq. 33 into Eq. 41, then assuming spherical geometry, a 1:1 electrolyte, and a cation activity coefficient of unity, we obtain

$$\frac{i_n}{F} = k_a \exp\left(\frac{2\gamma\overline{V}_M^{\alpha\prime}\alpha_m}{rRT}\right)\exp\left(\frac{\alpha_a F\Phi}{RT}\right) - k_c c_{M^+} \exp\left[-\frac{2\gamma\overline{V}_M^{\alpha\prime}(1-\alpha_m)}{rRT}\right]\exp\left(-\frac{\alpha_c F\Phi}{RT}\right) \quad [43]$$

The kinetic expression hypothesized in the extended Barton and Bockris propagation theory proposed by Diggle *et al.*[10] can be obtained by setting α_m equal to one. Then Eq. 43 reduces to

$$\frac{i_n}{F} = k_a \exp\left(\frac{2\gamma\overline{V}_M^{\alpha\prime}}{rRT}\right)\exp\left(\frac{\alpha_a F\Phi}{RT}\right) - k_c c_{M^+} \exp\left(-\frac{\alpha_c F\Phi}{RT}\right) \quad [44]$$

From Fig. 3 we can see that to choose this α_m value, implicit in the propagation theory development, involves an assumption that the activation peak is in a region with the mechanical properties of solution.

Though the mechanical transfer coefficient α_m adds an unknown parameter to our kinetic expression, its limited range of values, definite physical interpretation, independence of electrical effects, and ability to unify previously employed kinetic models (through clarification of their implicit assumptions) strongly argue for its inclusion. Experimental verification[12] of Oren and Landau's extension of propagation theory to growth of dendritic deposits in boundary layers, which employs a linearized form of Eq. 44, further suggests that a physical α_m value should be near one.

Now that the past models have been clarified, as a final step we should rearrange Eq. 40, replacing the parameters k_a and k_c with an exchange current density. First, we make the assumption that the cation activity coefficient in Eq. 39 is near unity

$$\frac{i}{z_+F} = k_a \exp\left(\frac{\alpha_a z_+F\Phi'}{RT}\right) - k_c c_{M^{z+}} \exp\left(-\frac{\alpha_c z_+F\Phi'}{RT}\right) \quad [45]$$

An open-circuit potential can be obtained from Eq. 45

$$V_0 = \frac{RT}{z_+F}\ln\left(\frac{k_c c_{M^{z+}}}{k_a}\right) \quad [46]$$

The exchange current density at an undeformed interface at constant concentration then takes the form

$$i_{0,ref} = z_+F k_a^{\alpha_c}(k_c c_{ref})^{\alpha_a} \quad [47]$$

and the kinetic equation reduces to

$$i_n = i_{0,\mathrm{ref}}\left(\frac{c_{M^{z+}}}{c_{\mathrm{ref}}}\right)^{\alpha_a}\exp\left[\frac{(\alpha_m - \alpha_a)z_+\Delta\mu_{e^-}^{\alpha,\alpha'}}{RT}\right] \times\left[\exp\left(\frac{\alpha_a z_+ F\eta_s}{RT}\right) - \exp\left(-\frac{\alpha_c z_+ F\eta_s}{RT}\right)\right] \quad [48]$$

Equation 48 can be used to give the effect of interfacial deformation on the measured exchange current density at any given time

$$i_0 = i_{0,\mathrm{ref}}\left(\frac{c_{M^{z+}}}{c_{\mathrm{ref}}}\right)^{\alpha_a}\exp\left[\frac{(\alpha_m - \alpha_a)z_+\Delta\mu_{e^-}^{\alpha,\alpha'}}{RT}\right] \quad [49]$$

Substitution of Eq. 34 into Eq. 49 shows how external pressure and viscous and elastic stresses in the electrode and electrolyte affect the exchange current density.

Effect of Mass-Transfer Limitations

To extend our kinetic model further, we should also take into account the fact that local mass-transfer limitations may occur near the roughening surface. For inclusion of these effects, we return to the sketch of phases shown in Fig. 1. Thus far, the quantity we have referred to as the surface overpotential has been given by

$$\eta_s = \Phi_1 - \Phi_2 - (\Phi_1 - \Phi_2)_{\mathrm{eq}} \quad [50]$$

where Φ_1 is the electric potential at the deformed electrode (phase α) and Φ_2 is the potential of an undeformed reference electrode (phase γ), contacting the bulk solution immediately adjacent to the surface (phase β). Because of the changes in current induced by roughening of the interface, we expect that the concentration in phase β does not necessarily match the one yielded by the macroscopic transport equations, which do not account for these local concentration deviations.

To be used in our development, macroscopic potentials should be related to local differences by exchanging η_s for a "macroscopic surface overpotential," η

$$\eta = \Phi_1 - \Phi_3 - (\Phi_1 - \Phi_3)_{\mathrm{eq}} = \eta_s + \Phi_2 - \Phi_3 - (\Phi_2 - \Phi_3)_{\mathrm{eq}} \quad [51]$$

The equilibrium term in Eq. 51 can be expressed as

$$F(\Phi_2 - \Phi_3)_{\mathrm{eq}} = \mu_{e^-}^{\varepsilon} - \mu_{e^-}^{\gamma} = \frac{\mu_{c_{M^{z+}}}^{\beta} - \mu_{c_{M^{z+}}}^{\delta}}{z_+} \quad [52]$$

Using constitutive Eq. 8 and including the liquid-junction potential $\Phi^\beta - \Phi^\delta$, we find that

$$(\Phi_2 - \Phi_3)_{\mathrm{eq}} = \frac{RT}{z_+F}\ln\left(\frac{f_{c_{M^{z+}}}^{\beta}c_{M^{z+}}^{\beta}}{f_{c_{M^{z+}}}^{\delta}c_{M^{z+}}^{\delta}}\right) + (\Phi^\beta - \Phi^\delta) \quad [53]$$

Typically, the liquid-junction potential is small; neglecting it, we obtain

$$\eta = \eta_s + \frac{RT}{z_+F}\ln\left(\frac{f_{c_{M^{z+}}}^{\beta}c_{M^{z+}}^{\beta}}{f_{c_{M^{z+}}}^{\delta}c_{M^{z+}}^{\delta}}\right) \quad [54]$$

Substitution of Eq. 54 into Eq. 48 gives

$$i_n = i_{0,\mathrm{ref}}\left(\frac{f_{c_{M^{z+}}}^{\delta}c_{M^{z+}}^{\delta}}{f_{c_{M^{z+}}}^{\beta}c_{\mathrm{ref}}}\right)^{\alpha_a}\exp\left[\frac{(\alpha_m - \alpha_a)z_+\Delta\mu_{e^-}^{\alpha,\alpha'}}{RT}\right] \times\left[\exp\left(\frac{\alpha_a z_+ F\eta}{RT}\right) - \left(\frac{f_{c_{M^{z+}}}^{\beta}c_{M^{z+}}^{\beta}}{f_{c_{M^{z+}}}^{\delta}c_{M^{z+}}^{\delta}}\right)\exp\left(-\frac{\alpha_c z_+ F\eta}{RT}\right)\right] \quad [55]$$

Table I. Assumptions employed in derivation of kinetic model.

1. Electrode is pure M	9.Butler-Volmer kinetics applies in the underformed state
2. System is isothermal	10. Transfer coefficients sum to unity
3. Concentrations unaffected by volume strain	11. Secondary reference state similar for phases α and β, independent of pressure
4. Molar volumes are relatively unaffected by volume strain	12. Activity coefficients constant or near unity
5. Surface energy is isotropic	13. Liquid junction potentials can be neglected
6. Dilatational resistance of the interface is neglected	14. No side reactions
7. Surface energy constant with respect to curvature	
8. Interfacial charge transfer is elementary and reversible	

Equation 55 allows incorporation of mass-transfer effects in electrolytes at moderate dilution. Under the assumption that activity coefficients take similar values in phases δ and β, we obtain a simpler expression

$$i_n = i_{0,\mathrm{ref}}\left(\frac{c_{M^{z+}}^{\delta}}{c_{\mathrm{ref}}}\right)^{\alpha_a}\exp\left[\frac{(\alpha_m - \alpha_a)z_+\Delta\mu_{e^-}^{\alpha,\alpha'}}{RT}\right] \times\left[\exp\left(\frac{\alpha_a z_+ F\eta}{RT}\right) - \left(\frac{c_{M^{z+}}^{\beta}}{c_{M^{z+}}^{\delta}}\right)\exp\left(-\frac{\alpha_c z_+ F\eta}{RT}\right)\right] \quad [56]$$

Note that the rationale employed to obtain this equation is less stringent than the ideal solution approximation, which requires activity coefficients to be near unity.

Equation 56 represents our desired goal. We have obtained a kinetic relationship which includes the effects of a general deformation through the term $\Delta\mu_{e^-}^{\alpha,\alpha'}$ and local deviations from macroscopic mass transfer through $c_{M^{z+}}^{\beta}$. Given initial conditions of specified interfacial roughness and $c_{M^{z+}}^{\beta} = c_{M^{z+}}^{\delta}$, all quantities in Eq. 56 can be evaluated in terms of macroscopically measurable thermodynamic and material properties by transient solution of the appropriate governing equations.

Conclusions

A relationship has been developed to describe the kinetics of roughening interfaces. All assumptions explicitly employed in this development are listed in Table I. The kinetic expressions employed in linear stability theory and the Barton and Bockris dendrite propagation model have been extended to incorporate mechanical effects other than the surface tension, including elastic, viscous, and external pressure forces. Each theory is consistent with the model developed here: the Barton and Bockris model is shown to assume that the activation peak for reaction is in a region with the mechanical properties of solution ($\alpha_m = 1$), and the linear stability approach is shown to assume that the exchange current density at a roughening interface is unaffected by deformation ($\alpha_m = \alpha_a$).

An elastic solid of high shear modulus, such as a cross-linked polymer electrolyte, is the strongest possible separator material one is likely to attain in a practical battery system. Future work will apply the general development provided here to the lithium/polymer system, employing linear elasticity theory to show how the elastic moduli of the polymer and lithium adjacent to an interface contribute to evolving surface shapes as current is passed.

Acknowledgments

This work was supported by the Assistant Secretary for Energy Efficiency and Renewable Energy, Office of FreedomCAR and Vehicle Technologies of the U.S. Department of Energy, under contract DE-AC03-76SF00098, and by the Shell Foundation.

The University of California, Berkeley, assisted in meeting the publication costs of this article.

List of Symbols

a_i	electrochemical activity of species i, mol/m^3
a_i^θ	property of species i dependent on the secondary reference state, m^3/mol
c_i	concentration of species i, mol/m^3
c_{ref}	reference concentration of cation, mol/m^3
$\underline{e}_n$	unit vector normal to the interface, unitless
$\underline{e}_t$	unit vector tangential to the interface, unitless
$E_{a,0}$	activation energy, J/mol
F	Faraday's constant, 96,487 C/equiv
$\underline{F}$	force per unit area vector, Pa
f_i	molar activity coefficient of species i, unitless
$\mathcal{H}$	mean curvature, m^{-1}
i	current density, A/m^2
i_0	exchange current density, A/m^2
$i_{0,ref}$	reference exchange current density, A/m^2
i_n	magnitude of current density normal to surface, A/m^2
$\underline{\underline{I}}$	unit tensor, unitless
k_a	anodic rate constant, mol/s
k_a	cathodic rate constant, m^3/s
p	pressure, Pa
r	dendrite tip radius, m
r_1	first principal radius of curvature, m
r_2	second principal radius of curvature, m
R	ideal gas constant, 8.3143 J/mol K
t_+^0	cationic transference number, unitless
t_-^0	anionic transference number, unitless
T	absolute temperature, K
V_0	open-circuit potential, V
$\overline{V}_i$	partial molar volume of species i, m^3/mol
z_+	valency of cation, equiv/mol
z_-	valency of anion, equiv/mol

Greek

α_a	anodic transfer coefficient, unitless
α_c	cathodic transfer coefficient, unitless
α_m	mechanical transfer coefficient, unitless
Φ	quasi-electrostatic potential in a deformed state, V
Φ'	quasi-electrostatic potential in an undeformed state, V
$\Phi^\beta - \Phi^\delta$	liquid-junction potential between phases β and δ, V
γ	surface energy, J/m^2
η_s	local surface overpotential, V
η	macroscopic surface overpotential, V
μ_i	electrochemical potential of species i, J/mol
ν_+	stoichiometric number of cation in neutral salt, unitless
ν_-	stoichiometric number of anion in neutral salt, unitless
$\underline{\underline{\sigma}}$	stress tensor, Pa
$\underline{\underline{\tau}}_d$	elastic deformation stress tensor, Pa
$\underline{\underline{\tau}}_\nu$	viscous stress tensor, Pa

Subscripts and superscripts

e^-	electron
electr	electrode
eq	equilibrium
M	metal
M^{z+}	cation
$M_{\nu_+}X_{\nu_-}$	neutral salt
X^{z-}	cation
S	solvent
sol'n	solution
α'	undeformed electrode
α	deformed electrode
β'	undeformed electrolyte, affected by transport
β	deformed electrolyte, affected by transport
δ	electrolyte, unaffected by deformation or transport
ε	planar reference electrode in electrolyte unaffected by deformation or transport

References

1. R. Selim and P. Bro, *J. Electrochem. Soc.*, **121**, 1457 (1974).
2. I. Epelboin, *J. Electrochem. Soc.*, **127**, 2100 (1980).
3. See references in N. Ibl and K. Schadegg, *J. Electrochem. Soc.*, **114**, 54 (1967).
4. A. R. Despic and K. I. Popov, in *Modern Aspects of Electrochemistry*, Vol. 7, B. E. Conway and J. O'M. Bockris, Editors, p. 199, Plenum Press, New York (1972).
5. B. Shraiman and D. Bensimon, *Phys. Rev. A*, **30**, 2840 (1984).
6. R. F. Voss and M. Tomkiewicz, *J. Electrochem. Soc.*, **132**, 371 (1985).
7. J.-N. Chazalviel, *Phys. Rev. A*, **42**, 7355 (1990).
8. J. L. Barton and J. O'M. Bockris, *Proc. R. Soc. London, Ser. A*, **268**, 485 (1962).
9. C. Chen and J. Jorné, *J. Electrochem. Soc.*, **137**, 2047 (1990).
10. J. W. Diggle, A. R. Despic, and J. O'M. Bockris, *J. Electrochem. Soc.*, **116**, 1503 (1969).
11. M. Dollé, L. Sannier, B. Beaudoin, M. Trentin, and J.-M. Tarascon, *Electrochem. Solid-State Lett.*, **5**, A286 (2002).
12. Y. Oren and U. Landau, *Electrochim. Acta*, **27**, 739 (1982).
13. C. Monroe and J. Newman, *J. Electrochem. Soc.*, **150**, A1377 (2003).
14. R. L. Deutscher and S. Fletcher, *J. Electroanal. Chem. Interfacial Electrochem.*, **164**, 1 (1984).
15. R. L. Deutscher and S. Fletcher, *J. Chem. Soc., Faraday Trans.*, **94**, 3527 (1998).
16. W. W. Mullins and R. F. Sekerka, *J. Appl. Phys.*, **34**, 323 (1963).
17. W. W. Mullins and R. F. Sekerka, *J. Appl. Phys.*, **35**, 444 (1964).
18. R. Aogaki and T. Makino, *Electrochim. Acta*, **26**, 1509 (1981).
19. R. Aogaki, *J. Electrochem. Soc.*, **129**, 2442 (1982).
20. L. Sundström and F. H. Bark, *Electrochim. Acta*, **40**, 599 (1995).
21. G. Feuillade and Ph. Perche, *J. Appl. Electrochem.*, **5**, 63 (1975).
22. J. Newman, *Electrochemical Systems*, 2nd ed., p. 34, Prentice-Hall, Englewood Cliffs, NJ (1991).
23. J. Newman and T. W. Chapman, *AIChE J.*, **19**, 343 (1973).
24. L. E. Malvern, *Introduction to the Mechanics of a Continuous Medium*, p. 77, Prentice-Hall, Englewood Cliffs, NJ (1969).
25. R. B. Bird, W. E. Stewart, and E. N. Lightfoot, *Transport Phenomena*, 1st ed., p. 79, John Wiley & Sons, New York (1960).
26. L. E. Scriven, *Chem. Eng. Sci.*, **12**, 98 (1960).
27. W. M. Deen, *Analysis of Transport Phenomena*, p. 580, Oxford University Press, New York (1998).
28. W. J. Moore, *Basic Physical Chemistry*, p. 409, Prentice-Hall, Englewood Cliffs, NJ (1983).
29. P. Arora, R. E. White, and M. Doyle, *J. Electrochem. Soc.*, **145**, 3647 (1998).
30. E. A. Moelwyn-Hughes, *The Kinetics of Reactions in Solution*, p. 1, Clarendon Press, Oxford (1933).
31. J. O'M. Bockris and A. K. N. Reddy, *Modern Electrochemistry*, Vol. 2, p. 976, Plenum Press, New York (1970).
32. M. D. Pritzker and T. Z. Fahidy, *Electrochim. Acta*, **37**, 103 (1992).